Chemical Science

ROYAL SOCIETY OF CHEMISTRY

EDGE ARTICLE

Published on 29 June 2026
Licensed under CC-BY-NC 4.0

Check for updates

Cite this: *Chem. Sci.*, 2026, **17**, 16259

All publication charges for this article have been paid for by the Royal Society of Chemistry

$PhSO_2CF_2H$ as a difluoromethylene bridge connecting electrophiles and electronically diverse alkenes

Yunlong Zhao, Kaidi Zhu, Feng Zhao, Yanxia Zhang, Chuanfa Ni and Jinbo Hu *

Received 12th June 2026
Accepted 26th June 2026

DOI: 10.1039/d6sc04911g

rsc.li/chemical-science

The difluoromethylene ($-CF_2-$) motif is highly valuable in pharmaceuticals, agrochemicals, and materials science due to its unique physicochemical properties. Herein, we present a broadly applicable strategy for the modular synthesis of CF_2-containing compounds by using difluoromethylene to bridge electrophiles and electronically diverse alkenes, with difluoromethyl phenyl sulfone ($PhSO_2CF_2H$) as the difluoromethylene source. Central to this approach is the activation of (phenylsulfonyl) difluoromethylated derivatives ($PhSO_2CF_2R$) by the excited-state Hantzsch ester anion (HE^-), which enables efficient generation of difluoroalkyl radicals under mild conditions. This method exhibits broad substrate scope, accommodating electron-rich, neutral, and deficient alkenes, as well as a wide range of difluoroalkyl sulfones derived from alkyl halides, cyclic sulfates, and carbonyl compounds. Furthermore, we developed a simplified operational protocol that circumvents the need for pre-preparation of $PhSO_2CF_2R$. Mechanistic studies support a radical pathway initiated by single-electron transfer between the photoexcited HE^- and $PhSO_2CF_2R$. Practical applications are demonstrated through gram-scale syntheses and late-stage modification of bioactive molecules and functional materials, establishing a versatile platform for constructing a wide range of difluoromethylene-containing compounds.

Introduction

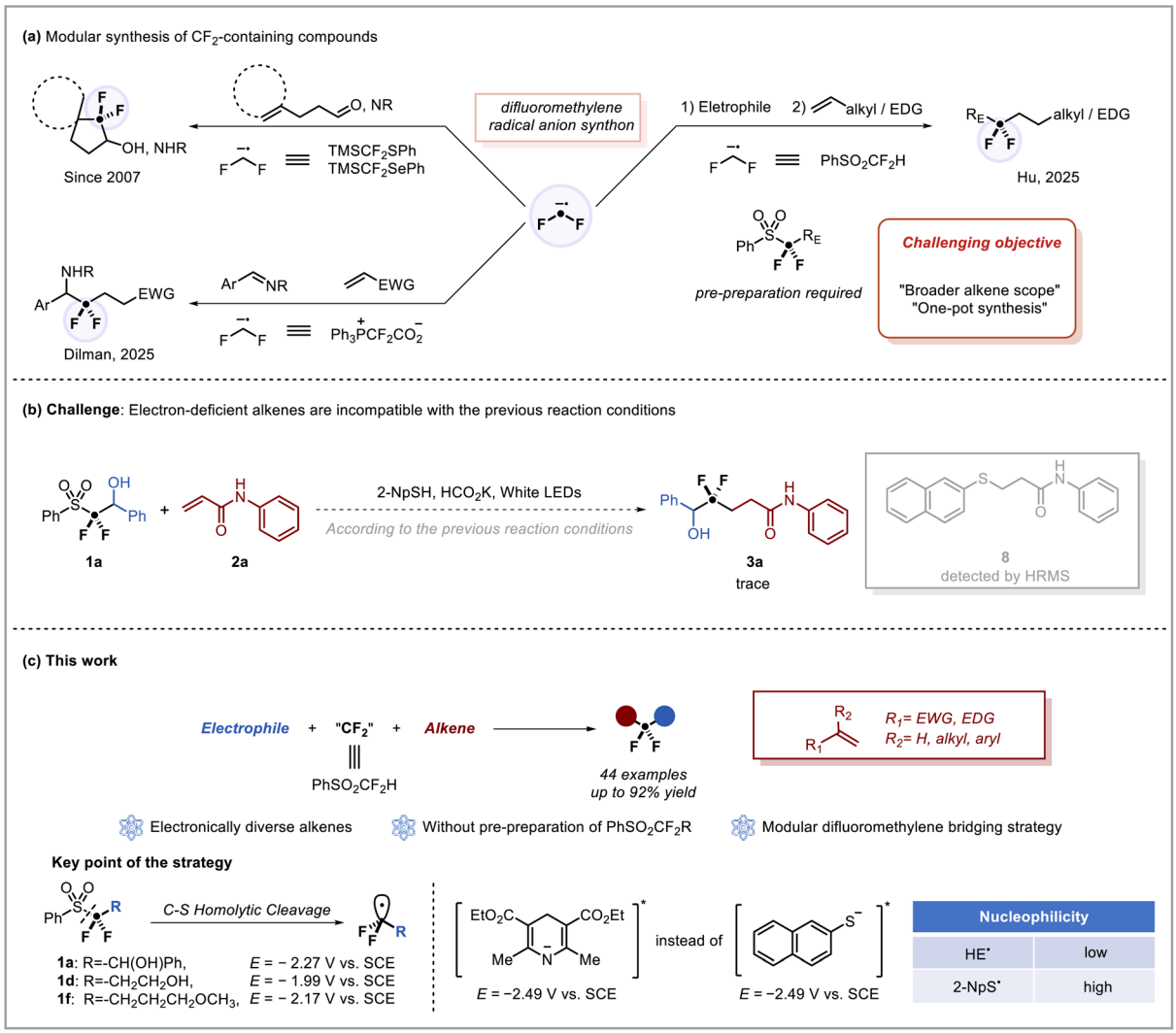
Fluorinated organic compounds have found broad applications in pharmaceuticals,[1,2] agrochemicals,[3] and materials,[4,5] owing to their ability to modulate key physicochemical properties, including metabolic stability, lipophilicity, and bioavailability. The difluoromethylene group ($-CF_2-$) serves as a versatile bioisostere of functional groups such as ether oxygens and carbonyls.[6] These unique properties have driven extensive research into the selective introduction of difluoroalkyl groups. The successful approval of drugs containing difluoromethylene units—such as voxilaprevir, tafluprost, and lenacapavir—further underscores the pressing need for simple and efficient strategies for selective difluoroalkylation. Accordingly, methods for the diverse construction of CF_2-containing compounds from simple, readily available precursors have thus become a major research focus.[7–10]

The modular construction of difluoromethylene-containing compounds primarily involves four synthetic intermediates (or synthons), including difluorocarbene,[11–13] difluoromethylene dianion,[14–17] difluoromethylene diradical,[18–20] and difluoromethylene radical anion. Among these, the difluorocarbene-based approach is limited by the direct interaction between electrophiles and nucleophiles, whereas difluoromethylene diradical and dianion species typically connect two functional groups of identical reactivity. In contrast, the difluoromethylene radical anion exhibits significant advantage in constructing structurally diverse difluoromethylene compounds, owing to the orthogonal reactivity of its substrates.[21] Since 2007, $TMSCF_2SPh$ and $TMSCF_2SePh$ have emerged as early examples of difluoromethylene radical anion synthons, predominantly applied in intramolecular cyclization reactions.[21–28] However, the second activation step of these reagents typically requires the highly toxic reducing agent nBu$_3$SnH. In 2025, the Dilman group developed a strategy in which an *in situ* generated difluorinated phosphorus ylide acted as a difluoromethylene radical anion synthon, facilitating the tandem reaction between electrophiles and radical acceptor molecules. Nevertheless, this approach suffers from significant limitations in substrate scope and is limited to the tandem reaction of imines and electron-deficient alkenes (Scheme 1a, left).[29]

Fluoroalkyl sulfones represent a class of fluorinated building blocks that exhibit both fluoroalkyl anion and fluoroalkyl radical characteristics. Fluoroalkyl aryl sulfones undergo single-electron reduction to generate fluoroalkyl radicals, which subsequently react with various radical acceptors such as isocyanides,[30] alkenes,[31–33] and thiols.[34] Meanwhile, the readily available difluoromethyl phenyl sulfone ($PhSO_2CF_2H$) serves as

State Key Laboratory of Fluorine and Nitrogen Chemistry and Advanced Materials, Shanghai Institute of Organic Chemistry, University of Chinese Academy of Sciences, Chinese Academy of Sciences, 345 Lingling Road, Shanghai 200032, China. E-mail: jinbohu@sioc.ac.cn

© 2026 The Author(s). Published by the Royal Society of Chemistry

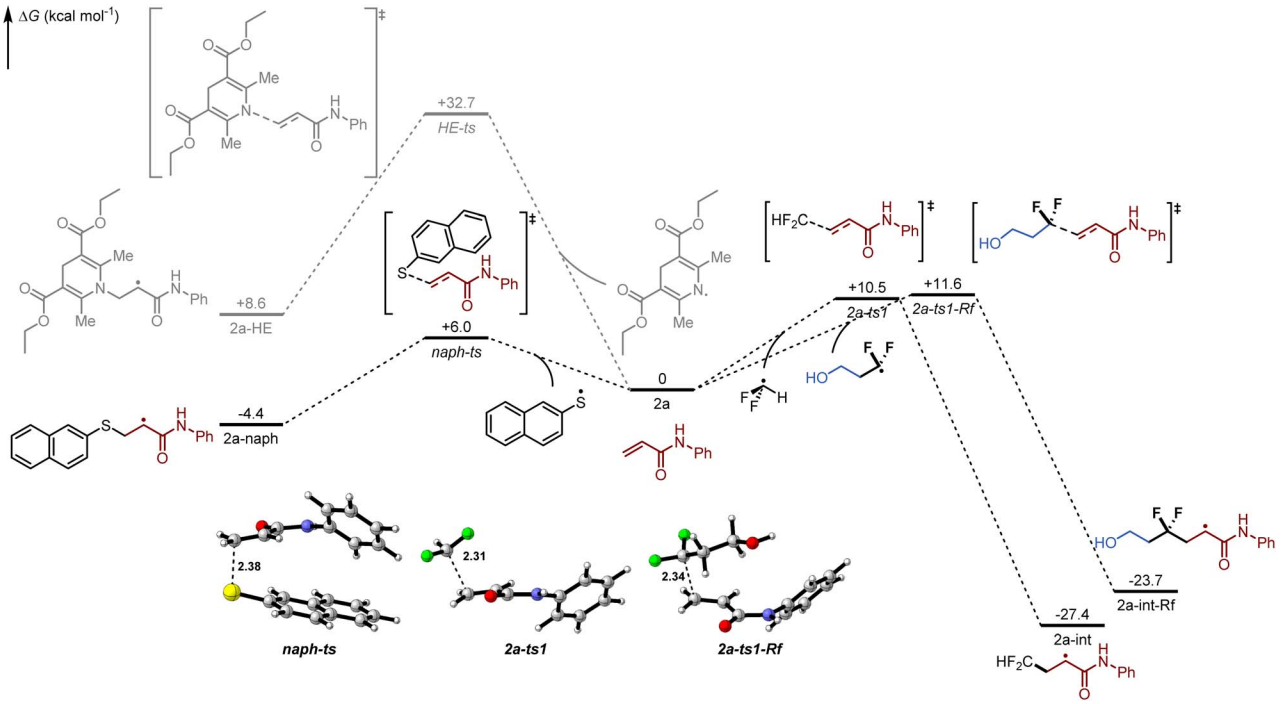


Scheme 1 Background and reaction design.

an effective nucleophilic difluoromethylating agent,[35,36] reacting with a broad range of electrophilic substrates—including aldehydes,[37] ketones,[38,39] imines,[40,41] alkyl halides,[42,43] and cyclic sulfates[44]—to furnish molecules bearing difluoromethyl (–CF_2H) or difluoromethylene (–CF_2–) functionalities. In these transformations, the phenylsulfonyl group functions primarily as a masking unit, modulating the nucleophilic reactivity of the $PhSO_2CF_2^-$ carbanion[45] and is removed through a two-electron process to afford the target functionalities. Recently, we used $PhSO_2CF_2H$ as a difluoromethylene radical anion synthon for the modular synthesis of CF_2-containing compounds with 2-naphthalenethiol (2-NpSH) and HCO_2K under photocatalytic conditions (Scheme 1a, right).[46] However, $PhSO_2CF_2R$ (Scheme 1a) required pre-preparation, which complicated the operational procedures. Meanwhile, the applicability of this strategy is mainly limited to electron-neutral and electron-rich alkenes,[46] while using electron-deficient alkenes sharply decreased the reaction efficiency (Scheme 1b, also see SI Fig. S2), and side products from 2-NpS$^\bullet$ addition to the alkene were observed, showing that the 2-NpS$^\bullet$ radical, besides acting as a HAT catalyst, also readily adds to the alkene, suppressing the desired reaction.

To support this hypothesis, we performed DFT calculations (Scheme 2). The results indicate that the energy barrier for the addition of 2-NpS$^\bullet$ to the alkene is +6.0 kcal mol^{-1}, which is lower than that for the addition of the difluoroalkyl radical ($RCF_2^\bullet$) to the alkene (+11.6 kcal mol^{-1}). These computational findings are consistent with the proposed explanation. To suppress these side reactions, it is necessary to develop a milder activation mode that is free from side reactions for the reduction of $PhSO_2CF_2R$. In previous studies, attempts were made to reduce $PhSO_2CF_2R$ using photocatalysts. However, the reaction efficiency was unsatisfactory when common photocatalysts such as 10-phenyl-10*H*-phenothiazine (PTH), 1,2,3,5-tetrakis(carbazol-9-yl)-4,6-dicyanobenzene (4-CzIPN), tris(2,2′-bipyridyl)ruthenium(II) chloride hexahydrate ($Ru(bpy)_3Cl_2\cdot 6H_2O$), and tris(2-phenylpyridine)iridium ($Ir(ppy)_3$) were employed.[46] We thus recognized that a reductant with a reduction potential similar to that of the excited-state 2-NpS$^-$ is necessary to achieve efficient reduction of $PhSO_2CF_2R$.

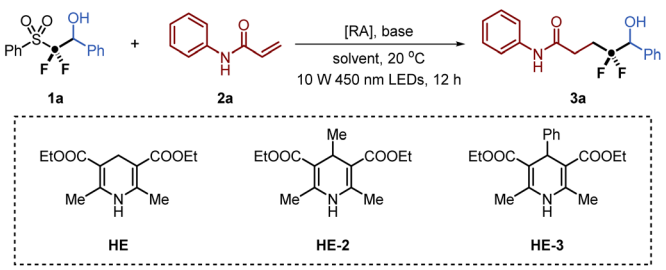
© 2026 The Author(s). Published by the Royal Society of Chemistry



Scheme 2 Computed Gibbs free energy profile of competing reaction pathways. Calculation methods: M06-2X/Def2-TZVPP/SMD(DMSO)//M06-2X/Def2-TZVP/SMD(DMSO). All bond lengths are in angstroms (Å).

It has been previously reported that the excited-state Hantzsch ester anion (HE^-) exhibits reducing power comparable to that of the excited-state 2-NpS^-.[46,47] From a structural perspective, the radical generated upon reduction of the Hantzsch ester ($HE^{\bullet}$) can directly serve as a hydrogen atom donor, a process driven by aromatization. The nitrogen-centered radical in this intermediate possesses significant steric hindrance, which likely reduces its tendency to add to alkenes. To support this view, we performed DFT calculations, which demonstrate that the addition of $HE^{\bullet}$ to alkenes is highly unfavorable both thermodynamically and kinetically (Scheme 2). Based on these results, we propose that HE can serve as a superior alternative to 2-NpSH for the reduction of $PhSO_2$-CF_2R. Meanwhile, previous studies have reported that HE can act not only as a hydrogen source in reactions but also facilitate single-electron reduction of substrates by forming electron donor–acceptor (EDA) complexes with electron-deficient substrates.[48–52] Our previous work demonstrated that perfluoroalkyl sulfones can act as electron acceptors, engaging in EDA interactions with electron-rich thiophenolates to generate perfluoroalkyl radicals under visible light irradiation.[34] We speculated that a potential EDA interaction between HE and $PhSO_2CF_2R$ might also facilitate single electron transfer (SET). Herein, we present a broadly applicable strategy that uses difluoromethylene to bridge electrophiles and electronically diverse alkenes for the modular synthesis of CF_2-containing compounds, with $PhSO_2CF_2H$ serving as the difluoromethylene source. This strategy is compatible with a wide range of electron-rich, neutral, and deficient alkenes and avoids the need for pre-preparation of $PhSO_2CF_2R$. Mechanistic studies

Table 1 Optimization of reaction conditions[a]



Entry[a]	Base	[RA]	Solvent	1a : 2a	Yield[b] [%]
1	Cs_2CO_3	HE	DMSO	1.5 : 1.0	43
2	**CsOAc**	**HE**	**DMSO**	**1.5 : 1.0**	**89**
3	K_2CO_3	HE	DMSO	1.5 : 1.0	43
4	DBU	HE	DMSO	1.5 : 1.0	82
5	CsOAc	HE-2	DMSO	1.5 : 1.0	n.d.
6	CsOAc	HE-3	DMSO	1.5 : 1.0	n.d.
7	CsOAc	HE	DMSO	1.3 : 1.0	84
8	CsOAc	HE	DMSO	1.0 : 1.0	73
9	CsOAc	HE	DMSO	1.0 : 1.5	75
10	CsOAc	HE	DMF	1.5 : 1.0	77
11	CsOAc	HE	NMP	1.5 : 1.0	52
12	CsOAc	HE	MeCN	1.5 : 1.0	39

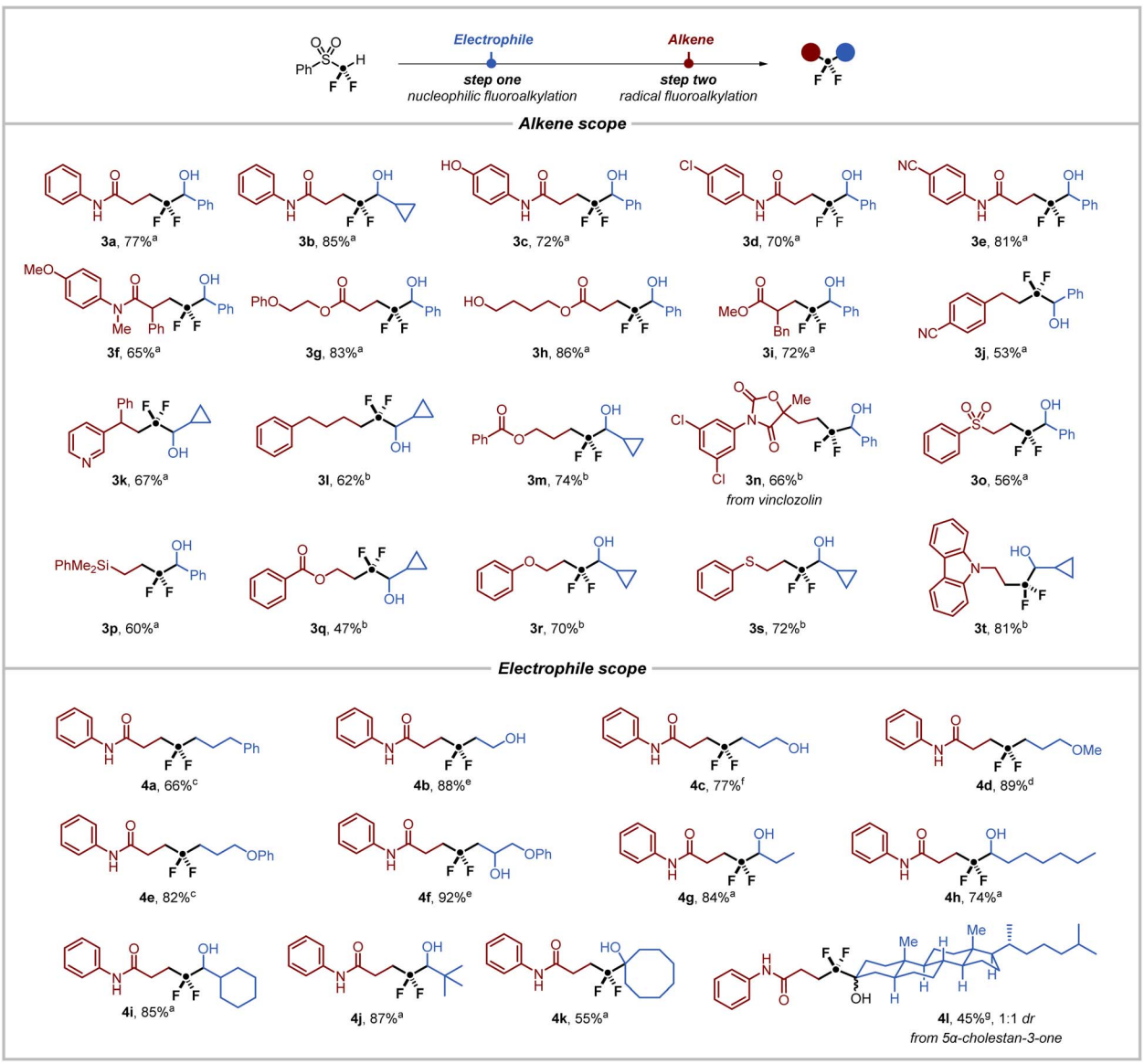
[a] Reaction conditions: **1a** (0.3 mmol, 1.5 equiv.), **2a** (0.2 mmol, 1.0 equiv.), HE (0.3 mmol, 1.5 equiv.), CsOAc (0.3 mmol, 1.5 equiv.), DMSO (2 mL); irradiated with 10 W 450 nm LEDs at 20 °C for 12 h. RA = reducing agent. [b] Yield was determined by ^{19}F NMR analysis using $PhOCF_3$ as an internal standard.

© 2026 The Author(s). Published by the Royal Society of Chemistry

show that photoexcitation of an HE–CsOAc complex triggers SET to $PhSO_2CF_2R$, generating the key difluoroalkyl radical ($RCF_2^{\bullet}$).

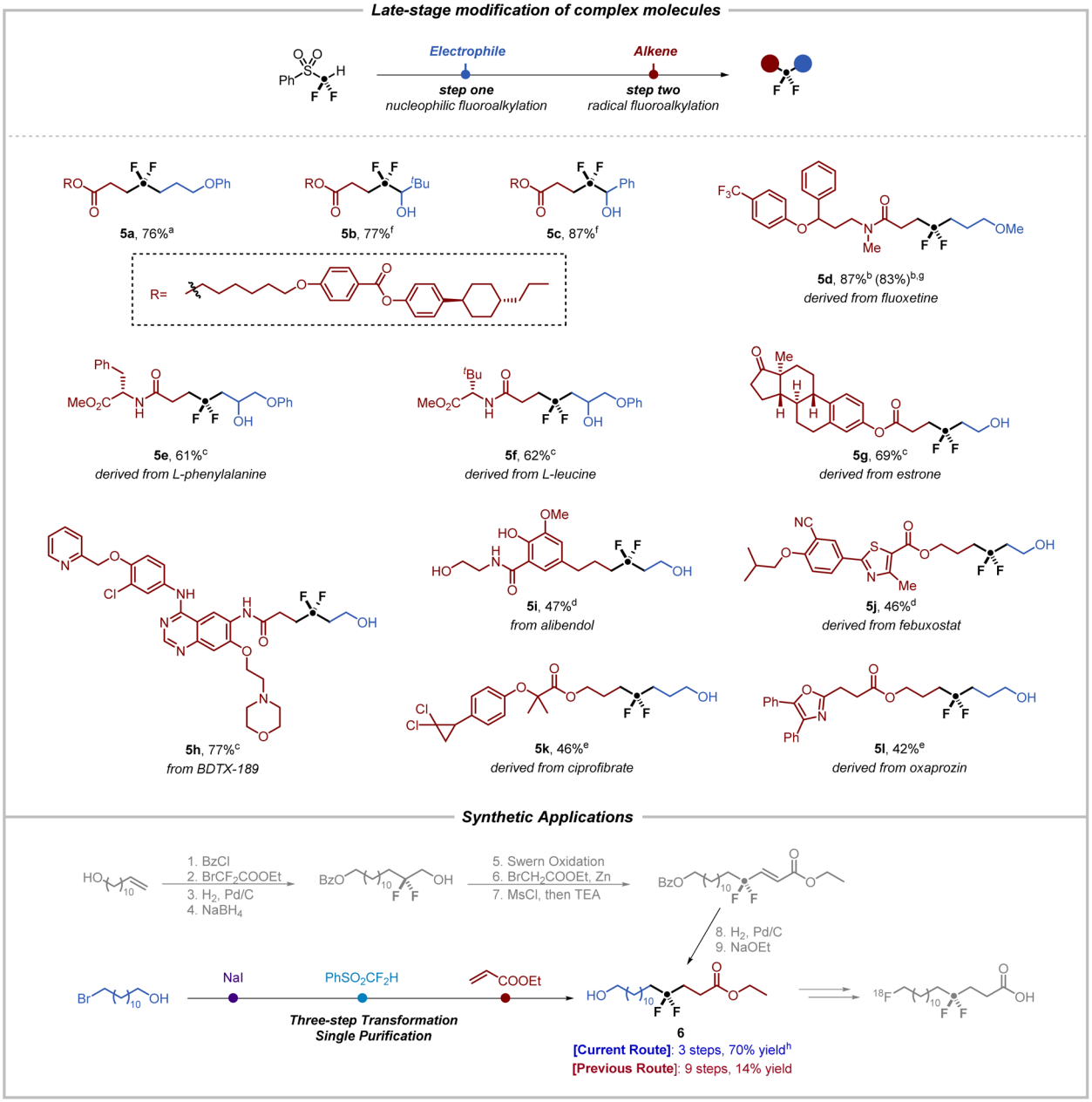
Results and discussion

To evaluate the efficiency of this strategy, we selected 2,2-difluoro-1-phenyl-2-(phenylsulfonyl)ethan-1-ol (**1a**) ($E = -2.27$ V *vs.* SCE) and *N*-phenylacrylamide (**2a**) as model substrates to investigate whether synergistic activation by HE and a base under blue LED irradiation could promote the hydrodifluoroalkylation reaction (Table 1). Initial screening showed that using DMSO as the solvent with HE and Cs_2CO_3 as additives under 450 nm irradiation for 12 h afforded the desired product in 43% yield, as determined by ^{19}F NMR analysis (entry 1). Subsequently, a series of common bases were screened to obtain the optimal reaction conditions (entries 2–4). Among these, CsOAc exhibited the highest activity and was selected as the optimal base for further studies. When the two alternative Hantzsch esters were used as the reducing agents in place of the standard Hantzsch ester (HE), no detectable amount of the desired product was obtained (entries 5–6); ^{19}F NMR spectroscopic monitoring revealed only minor conversion of **1a** (<15%). Subsequently, the stoichiometric ratio of the two substrates was systematically varied from 1.5 : 1.0 to 1.0 : 1.5 to probe its impact on reaction efficiency (entries 2 and 7–9). The optimal molar



Scheme 3 Substrate scope of the modular difluoromethylene bridging strategy. [a]Reaction conditions: alkene (1.0 equiv.), alkene : **1** : electrophile = 1.0 : 2.0 : 4.0; irradiated with 10 W 450 nm LEDs at 20 °C for 12 h. All yields are isolated yields and were calculated based on the amount of alkene. [b]Alkene : **1** : electrophile = 1.0 : 4.0 : 8.0. [c]Alkene : **1** : electrophile = 1.0 : 2.0 : 8.0. [d]Alkene : **1** : electrophile = 1.0 : 2.5 : 10.0. [e]Alkene : **1** : electrophile = 1.0 : 2.2 : 2.0. [f]Alkene : **1** : electrophile = 1.0 : 5.0 : 2.5. [g]Alkene : **1** : electrophile = 3.0 : 2.0 : 1.0, and yield was determined based on the electrophile.

© 2026 The Author(s). Published by the Royal Society of Chemistry



Scheme 4 Late-stage difluoroalkylation modification of complex molecules. [a]Alkene (1.0 equiv.), alkene : **1** : electrophile = 1.0 : 2.0 : 8.0, irradiated with 10 W 450 nm LEDs at 20 °C for 12 h. All yields are isolated yields and were calculated based on the amount of alkene. [b]Alkene : **1** : electrophile = 1.0 : 2.5 : 10.0. [c]Alkene : **1** : electrophile = 1.0 : 2.2 : 2.0. [d]Alkene : **1** : electrophile = 1.0 : 2.75 : 2.5. [e]Alkene : **1** : electrophile = 1.0 : 6.0 : 3.0. [f]Alkene : **1** : electrophile = 1.0 : 2.0 : 4.0. [g]Reaction was performed on a 3 mmol scale. [h]Yield was determined based on 12-bromo-1-dodecanol.

ratio of **1a** to **2a** was established as 1.5 : 1.0, which afforded the desired product in a maximum yield of 89%. Finally, the reaction was performed in a series of solvents with different polarities to elucidate solvent-dependent reactivity trends (entries 2 and 10–12). DMSO was identified as the optimal solvent owing to its excellent solubility for all reaction components. Through this sequential optimization, the optimal reaction conditions were established as follows: **1a** (1.5 equiv.), **2a** (1.0 equiv.), HE (1.5 equiv.), and CsOAc (1.5 equiv.) in DMSO (0.1 M) under irradiation with 450 nm blue LEDs for 12 h, which provided the highest yield (entry 2).

After optimizing the reaction conditions for the radical difluoroalkylation, we explored a convenient synthetic route starting from $PhSO_2CF_2H$. In initial attempts, when the crude product obtained by concentrating the organic phase from the previous anionic fluoroalkylation step was directly used the desired product **3a** could be detected. We hypothesized that this was due to residual benzaldehyde in the reaction system inhibiting the electron transfer process. Based on this, the

© 2026 The Author(s). Published by the Royal Society of Chemistry

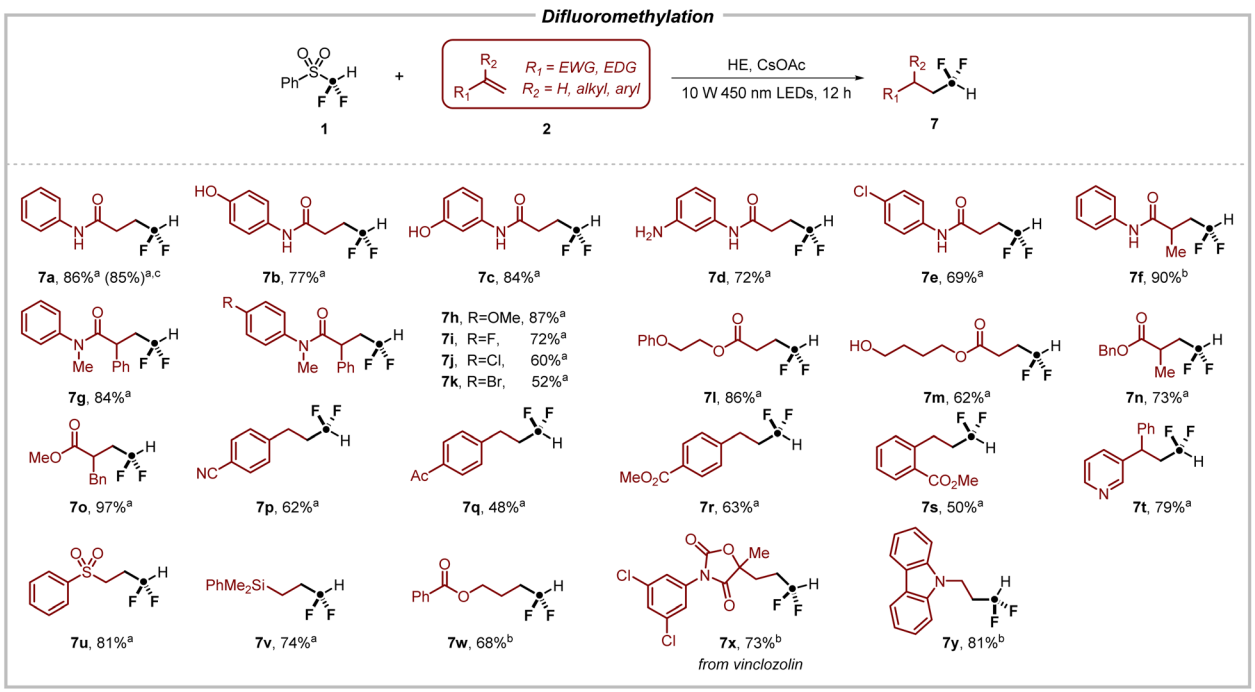
crude product from the first step was treated with an aqueous solution of sodium bisulfite ($NaHSO_3$) prior to the second radical fluoroalkylation step, ultimately affording the product **3a** in 77% isolated yield.

Having established the optimal reaction conditions, we next explored the alkene substrate scope of this method (Scheme 3). Gratifyingly, a wide range of electron-deficient alkenes, including various substituted acrylamides and acrylates (**3a–3i**), underwent the desired transformation smoothly with high efficiency. Notably, this protocol proved to be compatible with other alkenes of diverse electronic properties as well: aryl ethylenes substituted with electron-withdrawing groups (**3j** and **3k**), electron-neutral aliphatic alkenes (**3l–3n**), and heteroatom-substituted alkenes encompassing both electron-deficient and electron-rich variants (**3o–3t**). The broad substrate scope demonstrated here clearly highlights the significant synthetic potential and promising application prospects of this strategy for the efficient construction of structurally diverse CF_2-containing molecules.

Having established the alkene scope, we next examined the reactivity of $PhSO_2CF_2R$ derivatives generated *in situ* from a diverse array of electrophiles (Scheme 3), including alkyl halides (**4a**, **4d**, and **4e**), cyclic sulfates (**4b**, **4c**, and **4f**), aldehydes (**4g–4j**), and ketones (**4k–4l**). As anticipated, a broad range of structurally diverse $PhSO_2CF_2R$ were well tolerated under these conditions. Importantly, residual alkyl iodide electrophiles were removed by treating the crude product from the first step with DABCO, which forms insoluble quaternary ammonium salts, thereby preventing interference with the subsequent electron transfer process. Notably, a steroidal difluoroalkyl sulfone, prepared by nucleophilic addition to 5α-cholestan-3-one, also underwent efficient conversion (**4l**), highlighting the potential of this strategy for the installation of structurally complex difluoroalkyl groups.

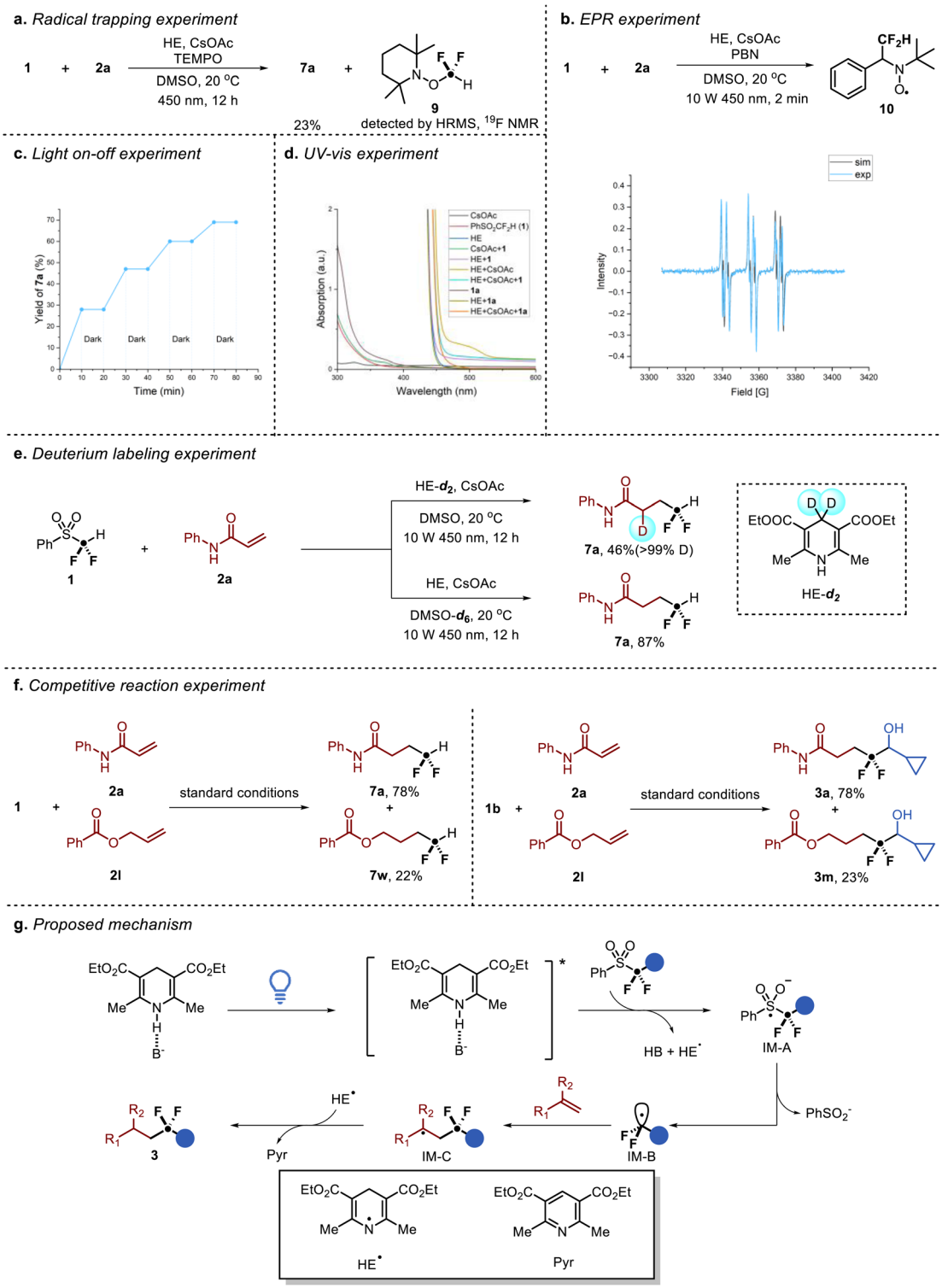
Given the high value of difluoromethylene motifs in pharmaceuticals, agrochemicals, and materials, we extended this strategy to the precision difluoroalkylation modification of functional molecules (Scheme 4). In liquid-crystal derivatives (**5a–5c**), targeted incorporation of difluoroalkyl segments modulated molecular polarity and self-assembly, offering a new route for the design of advanced liquid crystals with enhanced optoelectronic responses. The method also proved highly versatile for late-stage modification of bioactive molecules: fluoxetine derivative (**5d**), estrone derivative (**5g**), the EGFR inhibitor BDTX-189 (**5h**), alibendol (**5i**), febuxostat derivative(**5j**), ciprofibrate derivative (**5k**), oxaprozin derivative (**5l**), and several amino acid derivatives (**5e–5f**) underwent precise difluoroalkylation in moderate to excellent yields. Collectively, these results highlight the considerable potential of this strategy for the late-stage modification of diverse functional molecules.

To demonstrate the practical utility of this synthetic strategy, gram-scale reactions were performed. Under the scaled-up standard conditions, the fluoxetine derivative **4d** was obtained in a consistently high isolated yield of 83% (Scheme 4). This result confirms the robustness of the reaction system upon scale-up and highlights its significant practical value in synthetic chemistry. Notably, ^{18}F-labeled 4,4,16-trifluoropalmitic acid, a positron emission tomography (PET) tracer for myocardial fatty acid oxidation (FAO) imaging, has



Scheme 5 Substrate scope of alkene hydrodifluoromethylation. [a]Reaction conditions: alkene (1.0 equiv.), **1** (1.5 equiv.), DMSO (0.1 M), irradiated with 10 W 450 nm LEDs at 20 °C for 12 h. All yields are isolated yields and were calculated based on the amount of alkene. [b]Alkene (1.0 equiv.), **1** (3.0 equiv.). [c]Reaction was performed on a 5 mmol scale.

© 2026 The Author(s). Published by the Royal Society of Chemistry



Scheme 6 Mechanistic investigations and the proposed mechanism.

been accessed *via* a cumbersome synthetic route. The synthesis of its key precursor **6** requires a 9-step reaction sequence with an overall yield of only 14%.[53] In sharp contrast, our protocol enables access to precursor **6** in an excellent overall yield of 70% from commercially available 12-bromo-1-dodecanol *via* only 3 synthetic transformations and a single chromatographic purification. This dramatic improvement in synthetic efficiency further highlights the broad application potential of this methodology.

In addition to enabling the efficient construction of diverse difluoromethylene compounds, $PhSO_2CF_2H$ can also serve directly as a radical difluoromethylating agent for the

© 2026 The Author(s). Published by the Royal Society of Chemistry

hydrodifluoromethylation of various alkenes (Scheme 5). Diverse substituents—including halogens (**7e**, **7h**–**7k**, and **7x**), protic groups (**7b**–**7d** and **7m**), cyano (**7p**), and heteroaryl motifs (**7t** and **7y**)—were well tolerated, affording the desired products in moderate to excellent yields. Notably, aryl alkenes bearing electron-withdrawing substituents, whether monosubstituted or 1,1-disubstituted (**7g**–**7k** and **7p**–**7t**), underwent efficient conversion. The electron-deficient nature of sulfonyl and silyl substituents further activated the alkene moiety, enabling the vinyl sulfone and vinyl silane to be successfully converted in good yields (**7u** and **7v**). To probe the boundaries of substrate compatibility, electron-neutral alkene (**7w**), the agrochemical fungicide vinclozolin (**7x**), and electron-rich *N*-vinylcarbazole (**7y**) were examined. All of them reacted efficiently, underscoring the broad substrate scope of this method.

To elucidate the reaction mechanism, systematic investigations were carried out. Radical-trapping experiments showed significant suppression of product **7a** formation (Scheme 6a). High-resolution mass spectrometry (HRMS) detected the characteristic signal of the radical intermediate **9**. Taken together with the capture of radical species by electron paramagnetic resonance (EPR) spectroscopy at room temperature (Scheme 6b), these findings provide strong evidence for a radical pathway. Light on/off experiments revealed that **7a** is formed exclusively under continuous irradiation, thus ruling out a radical chain-propagation mechanism (Scheme 6c). To clarify the details of the photoinduced electron-transfer process, the interactions between the reaction components in solution were systematically examined by UV-vis absorption spectroscopy (Scheme 6d). Individual solutions of CsOAc or $PhSO_2CF_2H$(R) showed negligible absorption in the visible region, and no characteristic peaks were observed for binary mixtures of CsOAc with $PhSO_2CF_2H$ or $PhSO_2CF_2R$. In contrast, a solution of HE in DMSO displayed significant visible-light absorption. The spectrum remained largely unchanged upon addition of $PhSO_2CF_2H$(R) to HE. This suggests the absence of EDA complex formation between HE and $PhSO_2CF_2H$(R) and that the intermolecular electron transfer is instead attributed to the strong reducing capability of the excited-state Hantzsch ester anion. Deuterium-labeling experiments identified the hydrogen source: the use of deuterated HE (HE-d_2) led to high deuterium incorporation (>99%) in the product, whereas no significant incorporation occurred in deuterated solvent (DMSO-d_6). These results unequivocally confirm that HE also acts as the hydrogen donor (Scheme 6e). Competitive studies demonstrated that when electron-deficient and electron-neutral alkenes are simultaneously present, both difluoromethyl radicals and difluoroalkyl radicals preferentially add to electron-deficient alkenes (Scheme 6f). This phenomenon aligns with the known nucleophilic character of the difluoromethyl radical.[54]

Based on these mechanistic insights, we propose the following reaction pathway (Scheme 6g): photoexcitation of the EDA complex formed between HE and CsOAc generates the excited-state complex. Subsequent SET from the excited EDA complex to $PhSO_2CF_2R$ produces a sulfone radical anion (**IM-A**) and the HE$^{\bullet}$. Homolytic cleavage of the C–S bond in **IM-A** releases benzenesulfinate ($PhSO_2^-$), generating the corresponding difluoroalkyl radical (**IM-B**). Addition of **IM-B** to the alkene substrate affords the alkyl radical **IM-C**, which undergoes hydrogen-atom transfer from HE$^{\bullet}$ to deliver the product **3**, along with the formation of the aromatized pyridine derivative (Pyr). The potential energy surface of this reaction was also calculated, further supporting the proposed mechanism (for details, see Fig. S12 and S13 in the SI).

Conclusions

In summary, we have developed a modular strategy that uses difluoromethylene to bridge electrophiles and electronically diverse alkenes. $PhSO_2CF_2H$ serves as the difluoromethylene source, enabling the modular synthesis of CF_2-containing compounds. Mild activation of $PhSO_2CF_2R$ is achieved *via* a Hantzsch ester-CsOAc complex, enabling the generation of difluoroalkyl radicals under visible-light irradiation. The method exhibits remarkable substrate scope, accommodating electron-rich, neutral, and deficient alkenes, together with a diverse range of electrophiles (including alkyl halides, cyclic sulfates, and carbonyl compounds), highlighting its versatility for the installation of structurally diverse CF_2-containing compounds. The practical utility of this strategy has been demonstrated through gram-scale syntheses and late-stage difluoroalkylation of bioactive and functional molecules. The previously reported synthetic route for **6** was successfully modified with fewer steps and higher overall yield. This synthetic protocol promises to find more applications in the synthesis of important difluoromethylene-containing molecules.

Author contributions

Yunlong Zhao: data curation, investigation, methodology, writing – original draft. Kaidi Zhu: investigation, data curation, DFT calculation. Feng Zhao: data curation, investigation, validation. Yanxia Zhang: EPR measurement. Chuanfa Ni: discussion, funding, writing – review and editing. Jinbo Hu: supervision, funding, writing – review and editing.

Conflicts of interest

There are no conflicts to declare.

Data availability

The data that support the findings of this study are available in the supplementary information (SI) of this article. Supplementary information is available. See DOI: https://doi.org/10.1039/d6sc04911g.

Acknowledgements

This work was financially supported by the Strategic Priority Research Program of the Chinese Academy of Science (XDB0590000), the National Key Research and Development Program of China (2025YFA151110), the National Natural

© 2026 The Author(s). Published by the Royal Society of Chemistry

Science Foundation of China (22271299), and the Natural Science Foundation of Shandong Province (ZR2023LFG003). We gratefully acknowledge Professor Mingyou Hu for his valuable guidance and support. We also thank Shuo Sun, Haixia Song, Ling Deng, and Yi Luo for their technical assistance and helpful discussions during this work. We also acknowledge the computational resources provided by the HPC platform at ShanghaiTech University.

Notes and references

1 E. P. Gillis, K. J. Eastman, M. D. Hill, D. J. Donnelly and N. A. Meanwell, *J. Med. Chem.*, 2015, **58**, 8315–8359.
2 M. Inoue, Y. Sumii and N. Shibata, *ACS Omega*, 2020, **5**, 10633–10640.
3 T. Fujiwara and D. O'Hagan, *J. Fluorine Chem.*, 2014, **167**, 16–29.
4 M. Hird, *Chem. Soc. Rev.*, 2007, **36**, 2070–2095.
5 Z. Zhang, K. Chen, B. Ameduri and M. Chen, *Chem. Rev.*, 2023, **123**, 12431–12470.
6 N. A. Meanwell, *J. Med. Chem.*, 2018, **61**, 5822–5880.
7 D.-Q. Dong, H. Yang, J.-L. Shi, W.-J. Si, Z.-L. Wang and X.-M. Xu, *Org. Chem. Front.*, 2020, **7**, 2538–2575.
8 Z. Feng, Y. L. Xiao and X. Zhang, *Acc. Chem. Res.*, 2018, **51**, 2264–2278.
9 W. C. Fu, P. M. MacQueen and T. F. Jamison, *Chem. Soc. Rev.*, 2021, **50**, 7378–7394.
10 S. Barata-Vallejo, M. V. Cooke and A. Postigo, *ACS Catal.*, 2018, **8**, 7287–7307.
11 A. D. Dilman and V. V. Levin, *Acc. Chem. Res.*, 2018, **51**, 1272–1280.
12 X. Zeng, Y. Li, Q.-Q. Min, X.-S. Xue and X. Zhang, *Nat. Chem.*, 2023, **15**, 1064–1073.
13 Q. Xie and J. Hu, *Acc. Chem. Res.*, 2024, **57**, 693–713.
14 A. V. Alexandrova and P. Beier, *J. Fluorine Chem.*, 2009, **130**, 493–500.
15 M. D. Kosobokov, V. V. Levin, A. A. Zemtsov, M. I. Struchkova, A. A. Korlyukov, D. E. Arkhipov and A. D. Dilman, *Org. Lett.*, 2014, **16**, 1438–1441.
16 G. K. S. Prakash, J. Hu, T. Mathew and G. A. Olah, *Angew. Chem., Int. Ed.*, 2003, **42**, 5216–5219.
17 A. L. Trifonov and A. D. Dilman, *Org. Lett.*, 2021, **23**, 6977–6981.
18 V. S. Kostromitin, A. O. Sorokin, V. V. Levin and A. D. Dilman, *Chem. Sci.*, 2023, **14**, 3229–3234.
19 Z.-Q. Zhang, C.-Q. Wang, L.-J. Li, J. L. Piper, Z.-H. Peng, J.-A. Ma, F.-G. Zhang and J. Wu, *Chem. Sci.*, 2023, **14**, 11546–11553.
20 V. Reutrakul, T. Thongpaisanwong, P. Tuchinda, C. Kuhakarn and M. Pohmakotr, *J. Org. Chem.*, 2004, **69**, 6913–6915.
21 Y. Li and J. Hu, *Angew. Chem., Int. Ed.*, 2007, **46**, 2489–2492.
22 T. Bootwicha, D. Panichakul, C. Kuhakarn, S. Prabpai, P. Kongsaeree, P. Tuchinda, V. Reutrakul and M. Pohmakotr, *J. Org. Chem.*, 2009, **74**, 3798–3805.
23 K. Peewasan, C. Kuhakarn, D. Soorukram, P. Tuchinda, V. Reutrakul and M. Pohmakotr, *J. Fluorine Chem.*, 2012, **135**, 367–372.
24 W. Thaharn, D. Soorukram, C. Kuhakarn, P. Tuchinda, C. Pakawatchai, S. Saithong, V. Reutrakul and M. Pohmakotr, *J. Org. Chem.*, 2015, **80**, 816–827.
25 S. Keereewan, C. Kuhakarn, P. Leowanawat, S. Saithong, V. Reutrakul and D. Soorukram, *J. Org. Chem.*, 2022, **87**, 15963–15985.
26 G. Fourrière, J. Lalot, N. V. Hijfte, J.-C. Quirion and E. Leclerc, *Tetrahedron Lett.*, 2009, **50**, 7048–7050.
27 G. Fourrière, N. Van Hijfte, J. Lalot, G. Dutech, B. Fragnet, G. Coadou, J.-C. Quirion and E. Leclerc, *Tetrahedron*, 2010, **66**, 3963–3972.
28 G. Fourrière, E. Leclerc, J.-C. Quirion and X. Pannecoucke, *J. Fluorine Chem.*, 2012, **134**, 172–179.
29 G. A. Lozhkin, A. L. Trifonov and A. D. Dilman, *J. Org. Chem.*, 2025, **90**, 10148–10153.
30 J. Rong, L. Deng, P. Tan, C. Ni, Y. Gu and J. Hu, *Angew. Chem., Int. Ed.*, 2016, **55**, 2743–2747.
31 J. Rong, C. Ni, Y. Wang, C. Kuang, Y. Gu and J. Hu, *Acta Chim. Sin.*, 2017, **75**, 105–109.
32 Z. Wei, W. Zheng, X. Wan and J. Hu, *Angew. Chem., Int. Ed.*, 2023, **62**, e202308816.
33 L. Xiao, Z. Wei, C. Ni, A. D. Dilman and J. Hu, *Org. Lett.*, 2025, **27**, 1884–1888.
34 Z. Wei, Z. Lou, C. Ni, W. Zhang and J. Hu, *Chem. Commun.*, 2022, **58**, 10024–10027.
35 C. Ni, M. Hu and J. Hu, *Chem. Rev.*, 2015, **115**, 765–825.
36 J. Hu, *J. Fluorine Chem.*, 2009, **130**, 1130–1139.
37 G. P. Stahly, *J. Fluorine Chem.*, 1989, **43**, 53–66.
38 G. K. Surya Prakash, J. Hu, Y. Wang and G. A. Olah, *Eur. J. Org Chem.*, 2005, **2005**, 2218–2223.
39 M. Hu, B. Gao, C. Ni, L. Zhang and J. Hu, *J. Fluorine Chem.*, 2013, **155**, 52–58.
40 Y. Li and J. Hu, *Angew. Chem., Int. Ed.*, 2005, **44**, 5882–5886.
41 J. Liu, Y. Li and J. Hu, *J. Org. Chem.*, 2007, **72**, 3119–3121.
42 G. K. S. Prakash, J. Hu, Y. Wang and G. A. Olah, *Angew. Chem., Int. Ed.*, 2004, **43**, 5203–5206.
43 G. K. S. Prakash, J. Hu, Y. Wang and G. A. Olah, *Org. Lett.*, 2004, **6**, 4315–4317.
44 C. Ni, J. Liu, L. Zhang and J. Hu, *Angew. Chem., Int. Ed.*, 2007, **46**, 786–789.
45 C. Ni and J. Hu, *Chem. Soc. Rev.*, 2016, **45**, 5441–5454.
46 S. Sun, R. Jia, X. Zhou, Z. Wang, J. Rong, C. Ni and J. Hu, *Nat. Commun.*, 2025, **16**, 7731.
47 D.-L. Zhu, Q. Wu, H.-Y. Li, H.-X. Li and J.-P. Lang, *Chem.–Eur. J.*, 2020, **26**, 3484–3488.
48 J. Zhang, Y. Li, R. Xu and Y. Chen, *Angew. Chem., Int. Ed.*, 2017, **56**, 12619–12623.
49 Y. Jiang, Y. Wei, Q. Y. Zhou, G. Q. Sun, X. P. Fu, N. Levin, Y. Zhang, W. Q. Liu, N. Song, S. Mohammed, B. G. Davis and M. J. Koh, *Nature*, 2024, **631**, 319–327.
50 Q. Wang, B. C. Lee, T. J. Tan, Y. Jiang, W. H. Ser and M. J. Koh, *Nat. Synth.*, 2022, **1**, 967–974.
51 H. Y. Tu, S. Zhu, F. L. Qing and L. Chu, *Chem. Commun.*, 2018, **54**, 12710–12713.

© 2026 The Author(s). Published by the Royal Society of Chemistry

52 N. Li, J. L. Si and M. Y. Xu, *Chem.–Eur. J.*, 2025, **31**, e202404116.
53 A. Colombano, S. Dall'Angelo, L. Kingston, G. Grönberg, C. Correia, R. Passannante, Z. Baz, M. Á. Morcillo, C. S. Elmore, J. Llop and M. Zanda, *ChemMedChem*, 2020, **15**, 2317–2331.
54 M. Duan, Q. Shao, Q. Zhou, P. S. Baran and K. N. Houk, *Nat. Commun.*, 2024, **15**, 4630.

© 2026 The Author(s). Published by the Royal Society of Chemistry